8th U. S. National Combustion Meeting
Organized by the Western States Section of the Combustion Institute
and hosted by the University of Utah
May 19-22, 2013

Flammability Aspects of Fabric in Opposed and Concurrent Air Flow in Microgravity

Paul V. Ferkul[1] *Sandra L. Olson*[2] *Michael C. Johnston*[3] *James S. T'ien*[3]

[1]*National Center for Space Exploration Research, Cleveland, OH 44135*
[2]*NASA Glenn Research Center, Cleveland, OH 44135*
[3]*Case Western Reserve University, Cleveland, OH 44106*

Microgravity combustion tests burning fabric samples were performed aboard the International Space Station. The cotton-fiberglass blend samples were mounted inside a small wind tunnel which could impose air flow speeds up to 40 cm/s. The wind tunnel was installed in the Microgravity Science Glovebox which supplied power, imaging, and a level of containment. The effects of air flow speed on flame appearance, flame growth, and spread rates were determined in both the opposed and concurrent-flow configuration. For the opposed flow configuration, the flame quickly reached steady spread for each flow speed, and the spread rate was fastest at an intermediate value of flow speed. These tests show the enhanced flammability in microgravity for this geometry, since, in normal gravity air, a flame self-extinguishes in the opposed flow geometry (downward flame spread). In the concurrent-flow configuration, flame size grew with time during the tests. A limiting length and steady spread rate were obtained only in low flow speeds ($\leq$ 10 cm/s) for the short-length samples that fit in the small wind tunnel. For these conditions, flame spread rate increased linearly with increasing flow. This is the first time that detailed transient flame growth data was obtained in purely forced flows in microgravity. In addition, by decreasing flow speed to a very low value (around 1 cm/s), quenching extinction was observed. The valuable results from these long-duration experiments validate a number of theoretical predictions and also provide the data for a transient flame growth model under development.

1. Introduction

The combustion of thermally-thin fuels burning in low-speed flows has been studied extensively [e.g. Olson et al., 1988; Olson, 1991; Ferkul and T'ien, 1994; Grayson et al., 1994; T'ien and Bedir, 1997; Shih and T'ien, 1997]. The importance of radiative loss is evident in leading to flame extinction when the flow velocity (or ambient oxygen concentration) is reduced sufficiently. This quenching extinction occurs when the flame power output decreases, and the radiative heat loss rate becomes a significant fraction of the total combustion heat release from the flame.

The observation of the quenching extinction branch is only possible at microgravity, since otherwise any buoyant flow generated would take the system out of the low-speed flow regime. This is shown for a specific thermally-thin fuel in Fig. 1 produced by a computational model. A flame can only exist inside the U-shaped curve. The flammability boundary consists of two

branches, as shown. Normal gravity studies are limited to flow speeds above the minimum buoyant speed in the flame zone (20 cm/s for this system). The flames in microgravity are very sensitive to flow speed, especially as the flame approaches the extinction boundary. This has implications for both the fundamental understanding of mechanisms leading to diffusion flame extinction as well as practical significance for spacecraft fire safety. Materials in microgravity with adequate ventilation may burn more readily compared to normal gravity with all other conditions being identical (pressure, oxygen concentration, temperature, etc.).

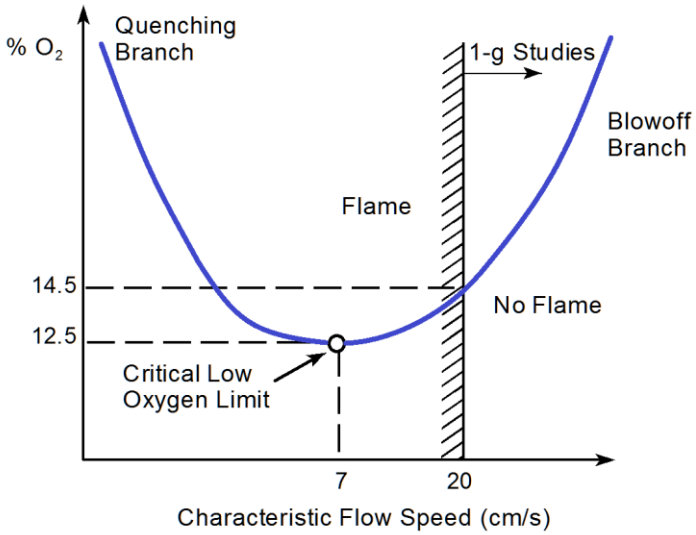

Figure 1. Flammability boundary for a thin solid fuel from model computation. Much of the boundary is inaccessible for study in 1-g because of the ever-present buoyant convection flows of at least 20 cm/s.

There have been few experiments examining concurrent-flow flame spread over thin fuels in the long-duration microgravity environments available in space. In Sacksteder et al. [1997], the number of tests was limited and only simple diagnostics were possible, but valuable insight into the burning behavior of thin paper samples was attained, including a visual record of the flames and measurements of spread rate and flame temperatures. The fuel tended to crack when it burned, causing the flame to respond in a non-predictable way. In Olson et al. [2001], ignition was initiated in the center of a paper fuel sheet so that only a portion of some of the flames spread in the concurrent mode. Depending on the flow speed, the flame would either spread entirely into the flow (opposed flow) or the ignition flame would split into an opposed and concurrent-flow flame spreading simultaneously away from each other.

Understanding long-duration microgravity solid material burning and extinction is important for improving strategies for NASA spacecraft materials selection. The goal is to link actual burn behavior in microgravity to Earth-based selection methods. From a more fundamental point of view, improved combustion computational models using the experimental results can be developed to aid in the design of fire detection and suppression systems both in microgravity and on Earth. Validated detailed combustion models in the simpler flow environment of microgravity can help build more complex combustion models of flames burning in normal gravity. Better models have wide applicability to the general understanding of many terrestrial combustion problems.

2. Methods

Combustion tests burning fabric sheets are conducted aboard the ISS (International Space Station) using the Microgravity Science Glovebox Facility [Butler, 2008]. The sheets are mounted in a holder which sandwiches the fabric between two thin stainless-steel frames. The exposed fuel measures 8.5 cm in length and 1 or 2 cm in width. One short edge of the fuel is not framed, and ignition is achieved across the sample on this edge. See Fig. 2. A 29-gage Kanthal wire spans the sample and is resistively heated to provide ignition. Typically the igniter resistance is 1 ohm and a current of around 3.7A is supplied for ignition, which occurs within about 2 s. The samples each

have their own integral igniter, the leads of which are glued flat along the frame to minimize any flow disturbances. The igniter leads come off the back of the sample and go to a connector which is plugged in during installation.

The custom-made fabric (sometimes referred to as SIBAL fabric) is a blend of cotton and fiberglass. The threads consist of fibers of cotton and fiberglass which are spun together. A simple weave patter is used with a spacing of 60 by 40 threads per inch (Fig. 3). The overall area density is 18.0 mg/cm^2, with 75% by mass cotton and remainder fiberglass. This fabric was developed with the idea that the fiberglass matrix would be left behind after all the fuel is consumed, so that the sheet would not curl or crack. Either of these geometrical changes could affect the flow in a non-predictable way and so are undesirable. As will be seen later, the flame is very sensitive to small air flow changes in microgravity.

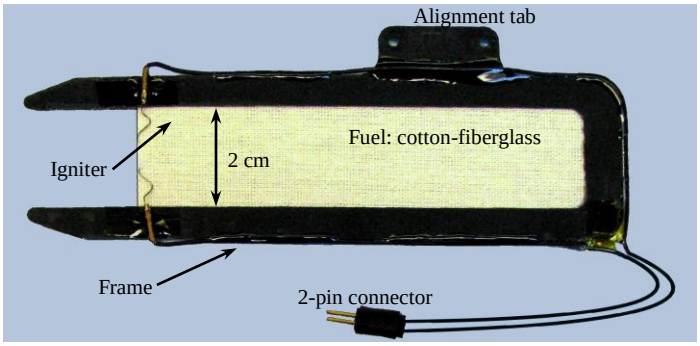

Figure 2. 2-cm wide fuel sample in holder. The open edge is ignited by a resistively heated wire. The igniter is terminated at a 2-pin connector which is plugged in when the sample is installed by the astronaut in the hardware.

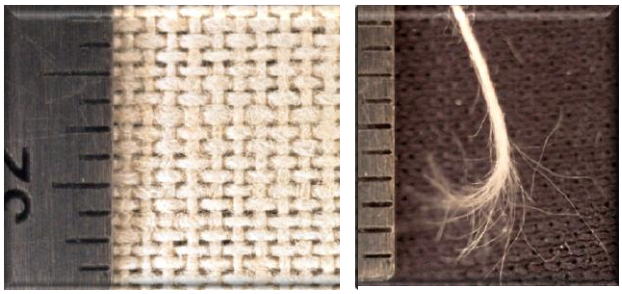

Figure 3. Left: Close-up of cotton-fiberglass fabric. A simple weave is used with a spacing of 60 x 40 threads per inch. Right: Each thread has cotton and fiberglass fibers intermingled.

The samples are burned in the SPICE apparatus which is a small flow duct with a cross-sectional area of 76mm x 76mm [Dotson et. al. 2010]. The front window of the duct can be opened so that samples can be installed one at a time. See Fig. 4. There is a tab with alignment holes on the sample holder which permits quick and accurate installation onto small rare-earth magnets inside the flow duct. Samples can be flipped 180 degrees so that the igniter is on the upstream or downstream end of the fuel. In this way, both concurrent-flow and opposed-flow tests can be conducted. The electrical connector is plugged into a socket inside the duct and the wires are tucked into a corner to minimize flow disturbances. A variable-speed fan is used to generate air flow speeds from 0 to 40 cm/s. Air speed is the principal variable for this experiment.

The flow duct is housed within the Microgravity Science Glovebox (MSG) which provides power, imaging, and a level of containment (Fig. 5) [Butler, 2008]. It is very advantageous that the astronaut can perform hands-on operation of the experiment while viewing the flame directly. Sometimes the flame is very dim or has features which the camera misses. The astronaut can make observations in real-time to the research team on the ground which is in direct audio and visual communication. The researchers on the ground in turn provide guidance and clarification is being performed while at the same time benefitting enormously from the direct involvement of the ISS crew member.

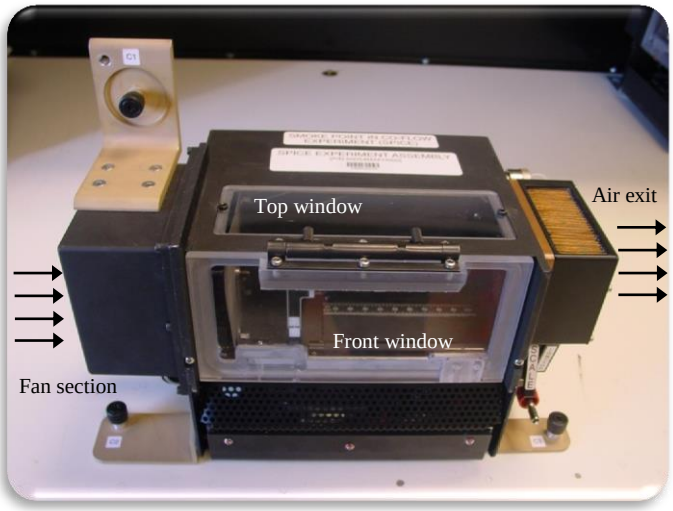

Figure 4. Small flow duct used to burn samples. The front window can be opened for easy installation of each fuel sample.

After all the appropriate electrical connections are made between the duct and the MSG, the cameras are set up. The cameras provide the bulk of the data for this experiment. A digital still camera takes high-resolution pictures through the top window at rate of about one frame per second. A video camera captures the edge view of the flame through the front window at 30 frames per second. There is a character overlay on the video image to display fan setting, flow speed (from a hot-wire anemometer), radiometer output from a wide-angle sensor inside the duct, and time.

After the sample is installed, the MSG volume is sealed and the lights are turned off. The experiment is operated using a control box which is external to the MSG and can adjust flow speed, igniter on/off, and radiometer gain. In addition to the camera views which are available live to both the astronaut and the ground team, the astronaut can look into a port to view the flame directly.

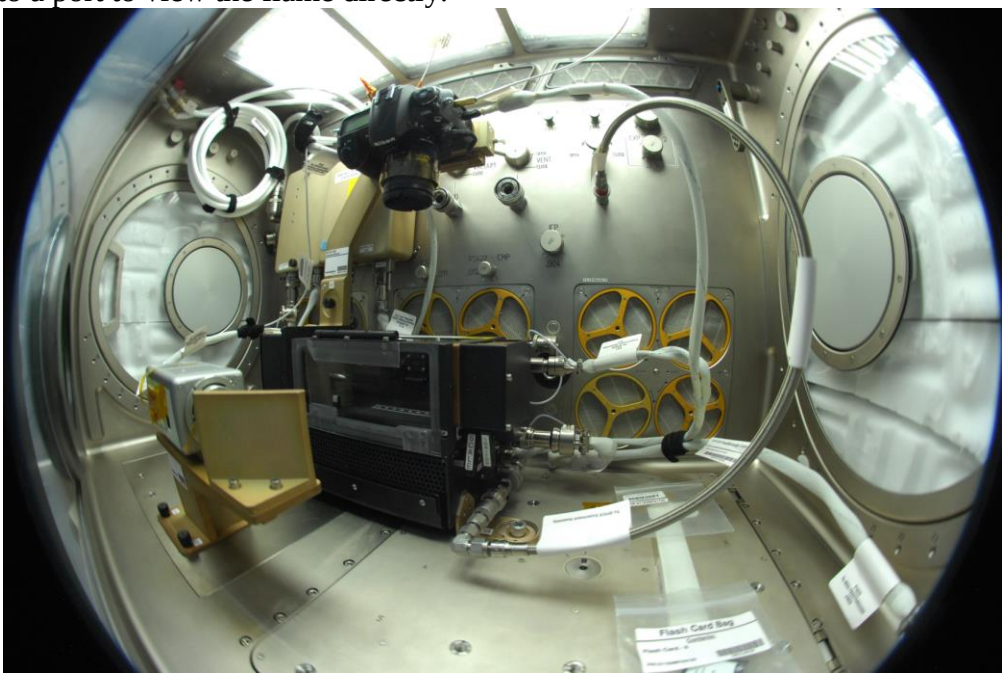

Figure 5. Fish-eye view of the inside of the Microgravity Science Glovebox (MSG) with the flow duct installed. The MSG provides power, imaging, and a level of containment. The astronaut can easily access the hardware which permits valuable hands-on operation. The digital still camera can be see viewing down at the duct, and a video camera and mirror image the sample through the front window.

Just before the test is initiated, the flow is set to the desired value and the cameras start recording. Ignition is turned on and a flame is established within about 2 seconds. The flame spreads across the sample, ultimately consuming all the fuel and then goes out. In some tests, the flow speed is changed while the flame is burning to gage its effect. After the flame goes out, the

duct is allowed to cool and vent for several minutes until the old sample can be removed and a fresh one installed for the next test.

3. Results and Discussion

Figure 6 shows typical flame images from both cameras for a concurrent-flow test at 10 cm/s and a 2-cm wide fabric. On the left, the digital still high-resolution image is shown looking down through the top window. The flame leading edge is mostly blue, but there is a significant amount of yellow which indicates the presence of soot. Dark charring on the surface is visible indicating the area of significant fuel pyrolysis. The base of the flame advances, leaving behind mostly fiberglass but with some remnants of cotton. This is evident by the bright orange smoldering occurring in the fuel matrix. Eventually, the smoldering ceases. On the right, the view of the flame from the front window video camera is shown. This view is important for determining flame symmetry and 2-D structure. While this camera lacks the sensitivity and resolution of the digital still camera, it records images at a much higher rate of 30 frames per second. For all cases, the two flame halves were symmetric and the flame spread uniformly without any disturbances caused by fuel burnout (cracking or curling). The text overlay indicates the fan setting, flow speed, radiometer level, date, and time. The minimum measurable air flow speed is 1 cm/s.

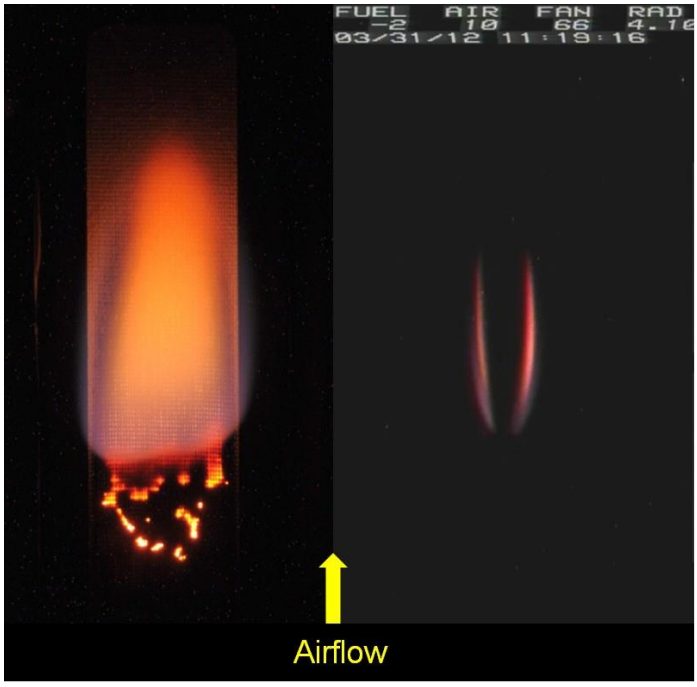

Figure 6. Typical flame images. Left: Digital still image from the top window looking down on the fabric sheet. Right: Edge view from the video camera viewing the flame through the front window. Video overlay information is shown at the top right. Flow speed direction is as indicated yielding a concurrent-flow configuration. (Test 1)

A total of 11 samples were available as shown in Table I. The tests are listed in the order in which they were performed.

Table I: Test Summary

Test	Width (cm)	Direction	Flow Speed (cm/s)	Comments
1	2	Concurrent	10, 5	Single flow speed change
7	2	Concurrent	10	
8	2	Concurrent	5	
4	2	Concurrent	22	
10	1	Concurrent	11	
5	2	Concurrent	5, 3, 1.5, 1	Flow reduction; quenching extinction observed
6	2	Opposed	9	
2	2	Concurrent	9, 44	Flow increase; blowoff extinction not attained
3	2	Opposed	10, 20, 44	Flow increase; blowoff extinction not attained
11	1	Concurrent	20	
9	2	Opposed	10, 6, 4, 2, 1.5, 1	Flow reduction; extinction not observed

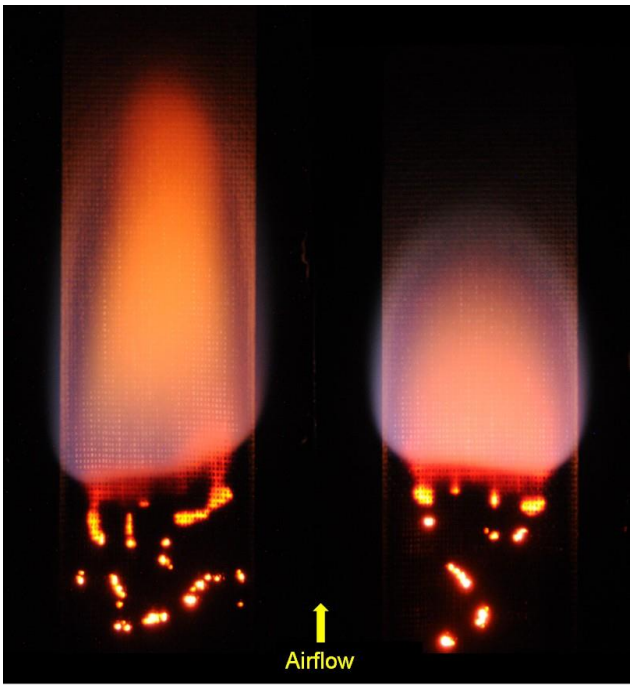

Figure 7. Effect of concurrent-flow speed on flame structure. Left: 10 cm/s. Right: 5 cm/s. (Tests 7 and 8)

Most of the samples were 2 cm in width, and most of the tests were performed in the concurrent-flow configuration. The opposed flow configuration was amenable to air flow speed changes during the burn since the flame was found to reach steady state quickly after the flow was changed. This is not the case for concurrent flow where the flame response time (and fuel length required) is significantly larger.

Figure 7 shows the comparison of concurrent air flow speeds of 5 and 10 cm/s on flame structure for a 2-cm wide sample. The images are taken about 20 seconds after ignition. The flame base for the wider samples in concurrent flow is rarely horizontal; rather there is always a slight tilt. The spread rate of the base of the flame does reach steady state during the available observation times for air flow speeds of 20 cm/s and less. However, the flame tip spread rate is still growing for air flow speeds equal to and higher than 10 cm/s. To put it another way, the flames only reach a steady length for flow speeds less than 10 cm/s.

In Fig. 8, a summary of the spread rates is presented. Results are plotted for both opposed flow (velocity > 0) and concurrent flow (velocity < 0). For opposed flow, the flame responds very rapidly to flow changes and steady state flame spread rates and lengths are obtained. As a result, a single burn can yield multiple data points if the flow is changed in a step-wise fashion. For concurrent flow, the flame takes a relatively long time to respond to flow changes so it is not feasible to attempt to get multiple data points per burn by changing flow speed. For concurrent flow, the flame base spread rate is plotted and reaches a steady state for all points shown. However the flame tip spread rate was increasing for the 2-cm wide samples above 5 cm/s air flow speed. The concurrent-flow flames burning the 1-cm wide samples did however reach a steady length.

Concurrent-flow flame spread rate increases linearly with flow speed, and linear curve fits are shown. Spread rate is width-dependent for the two widths studied. For concurrent flow, extinction was observed at a low but finite flow speed of less than 1 cm/s (shown by the dashed vertical line). Opposed-flow flame spread rate increases with flow to a maximum when the flow speed is around 10 to 15 cm/s and then decreases at higher speeds, in good agreement with previous research [Olson, 1991]. An opposed flow extinction test was attempted by decreasing the flow in a stepwise fashion, however extinction was not observed before the flame reached the end of fuel. Based on the trends however, it appears that an opposed-flow quenching extinction limit can be extrapolated to exist at an air flow speed of less than 1 cm/s. This implies that for this fuel, there is a small range of flow speeds near zero within which the flame cannot be sustained in either direction (concurrent or opposed).

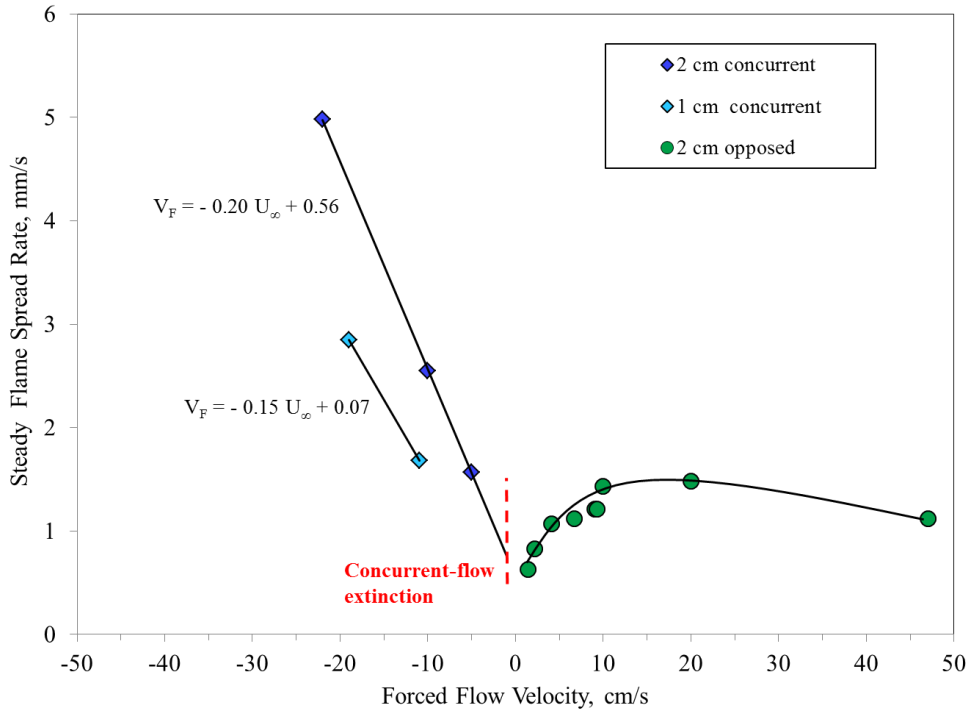

Figure 8. Summary of steady spread rates. For concurrent flow, steady flame base spread rates are reported. The red-dashed vertical line indicates concurrent-flow quenching extinction is achieved when air flow speed drops to less than 1 cm/s.

The flame spread measurements are made by tracking the flame base and tip position from the recorded images. The resolution and picture quality of the digital still images are far better than the video images. However, both can be used to determine flame spread rate. A sample tracking plot derived from the digital still images is shown in Fig. 9. The case shown is for a 1-cm wide sample burning in a concurrent flow of 11 cm/s. Ignition occurs at t=0. There is some initial development time when the flame grows, but after about 20 seconds the flame reaches steady state. This is obvious as the slopes of the base and tip positions become parallel for about 30 seconds and the flame length becomes constant. Furthermore, the visual images indicate the flame shape and intensity become nearly invariant during this period. Finally, when the flame runs out of fuel, it shrinks and goes out.

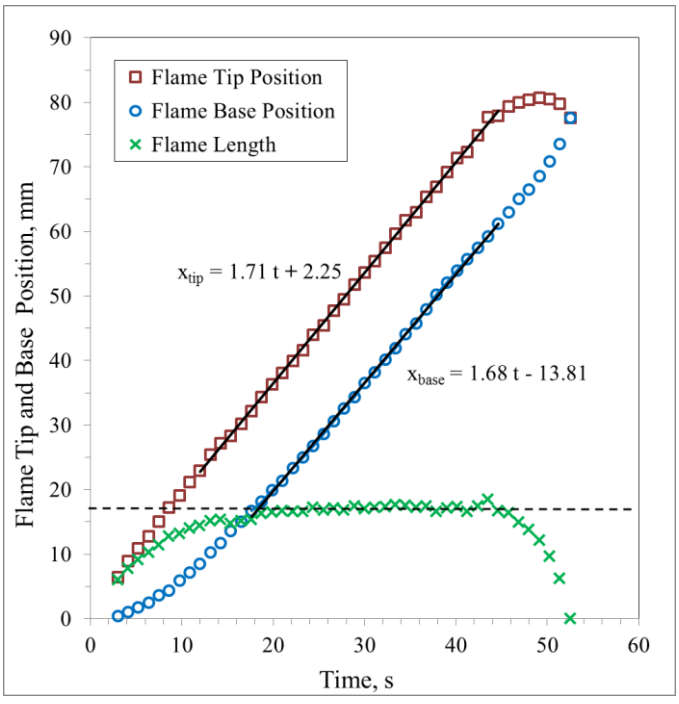

Figure 9. Flame growth to steady state spread for 1 cm sample width in concurrent air flow of 11 cm/s. (Test 10)

The opposed-flow flames all reach a steady length and spread rate as long as the air flow speed is held constant for around 5 seconds. The 1-cm wide concurrent-flow

flames also all reach a steady state. The concurrent-flow flames burning the 2-cm wide samples all have constant flame base spread rates over the available test duration. However, only air flows less than 10 cm/s yield steady flame lengths. The concurrent tests performed right at 10 cm/s give

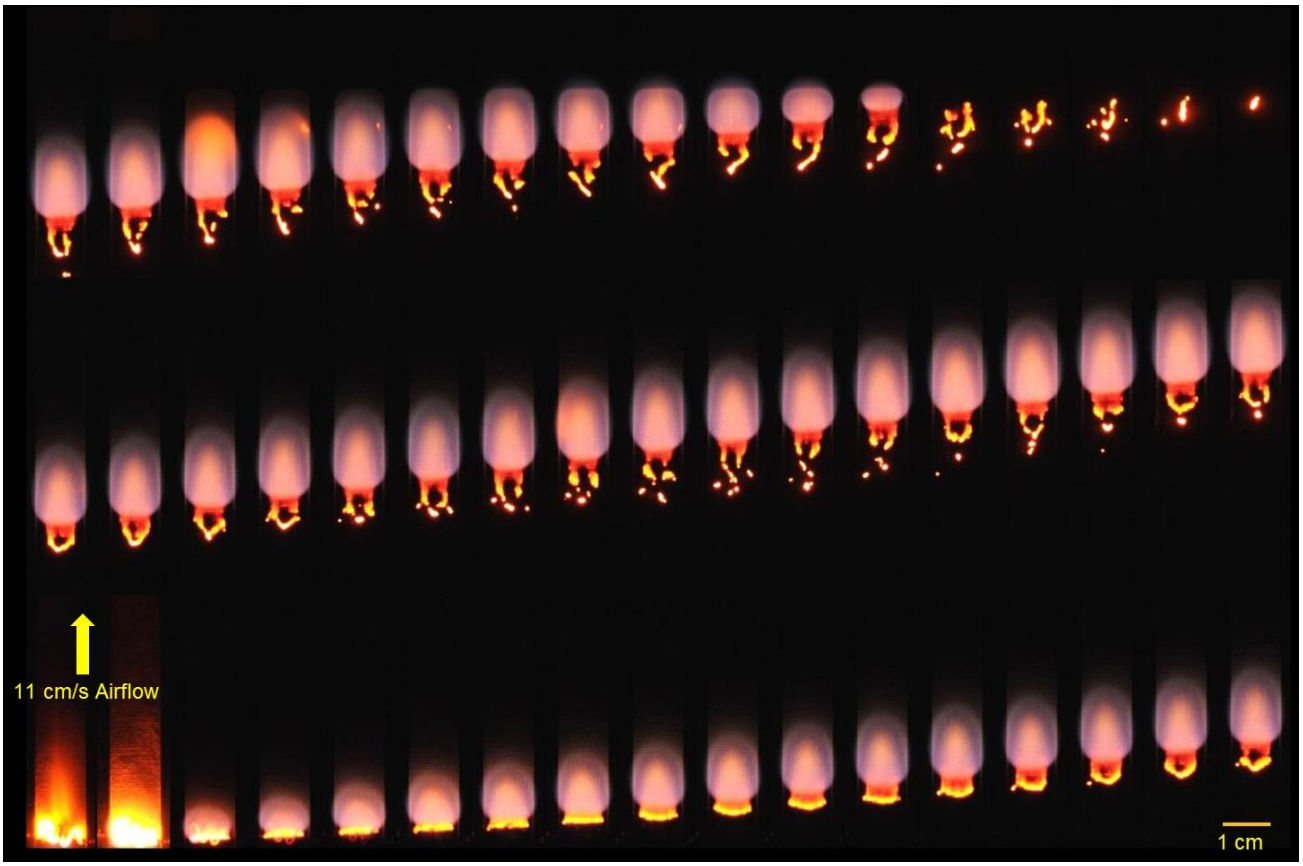

Figure 10. Digital still camera images for 1-cm-wide fuel with concurrent air flow = 11 cm/s. Images are taken every 1.125 sec (starting at bottom and moving from left to right). The flame reaches steady state after about 10 seconds. (Test 10)

indications that the flames are approaching a steady length, but the fuel samples are too short to conclude this with certainty.

In Fig. 10, the still image sequence is shown for 1-cm wide fuel sample in 11 cm/s concurrent air flow. The ignition, flame development, steady state spread, and extinction portions of the burn can be seen. In addition, the flames tend to leave behind a small amount of fuel when they spread. Since the fuel is very hot and now exposed to fresh oxygen, there is the development of an interesting pattern of smoldering visible as a bright orange glow in the fuel matrix beneath the flame. This surface reaction may have some effect on the stabilization of the flame.

For concurrent-flow flames, the fuel preheating depends on the entire flame and hot plume which means that the flame response time to flow changes is a strong function of the flame size. On the other hand, opposed-flow flames tend to respond quickly to flow changes since the fuel preheating ahead of the flame (which controls spread) only depends on the small region around the stabilization zone. One can take advantage of this aspect by performing a series of step-wise flow changes to get the spread behavior as a function of flow speed in a single test. In Fig. 11, the flame images from such a test are shown for a 2-cm wide sample burning in opposed flow. The flow is decreased from

10 cm/s all the way to nearly zero, and the spread rate is measured at each set flow speed. From this single burn, six different conditions are studied. The flow speed changes are indicated in the figure. The flame responds within a couple seconds, but the flame is allowed to burn at this speed for about 10 to 15 seconds so that a good spread rate determination can be made.

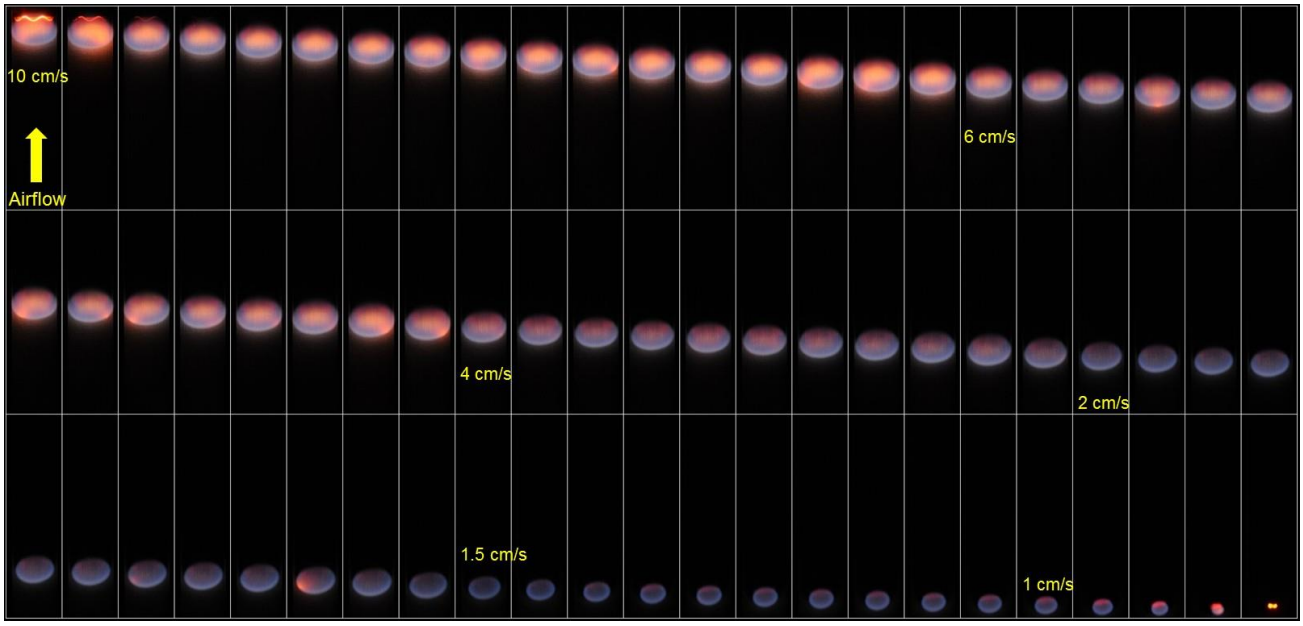

Figure 11. Digital still camera images showing a flame burning a 2-cm wide cotton-fiberglass fabric in opposed flow. Images are taken every 1.25 sec (starting at top and moving from left to right). The flow is decreased in discrete steps from 10 cm/s all the way down to less than 1 cm/s. The flame response to flow changes is very rapid, and the flow effects on the flame and its spread rate are dramatic. Total burn time is 90 sec. Flow changes are indicated by numbers. (Test 9)

One of the goals of his test was to determine the flow speed at which the flame would go out. Unfortunately, the flame went out because it simply ran out of fuel. The lowest flow imposed was less than 1 cm/s and the flame took on a nearly circular shape as diffusion of oxygen from all directions became increasingly important. Given the character of the flame at these very low flow speeds and the fact that this fuel will not burn at zero flow, it is reasonable to conclude that the flame will reach quenching at some finite (but small) flow speed.

In Fig. 12, the comparison of flow direction on a flame in microgravity is shown for a 2-cm wide fuel sample. The air flow speed is around 10 cm/s. The concurrent-flow flame is longer and spreads twice as fast as the opposed-flow flame. However, there is some indication from other experiments and models that at lower flow speeds, the opposed-flow flame will actually spread faster. It should be noted that although the opposed-flow flame looks brighter, this is likely due to the different camera settings used for the two tests.

As mentioned earlier, the concurrent-flow flame spread is controlled by the entire length of the hot flame and the opposed-flow flame only by its stabilization zone. Fig. 12 helps to visualize this effect. Also, note that there is no visible smoldering in the opposed-flow flame. This suggests that the flame is more completely pyrolyzing the fuel.

In Fig. 13, a comparison is made for two flames burning in concurrent flow, but with one in microgravity and the other in normal gravity. The microgravity flame has a convex base and nearly reaches a steady-state condition. The normal-gravity flame is much longer, sootier, has a concave base, and is still accelerating over the fuel length available. Observations and comparisons like this can help to guide model development of fundamental gravitational effects on flames. Also, these provide a useful assessment of normal-gravity test protocols used for the selection of fire-safe materials for spacecraft. The standard test used by NASA to rate materials relies on burning them in an upward, normal-gravity configuration [NASA, 1998]. Building the database of long-duration microgravity combustion tests will improve the understanding and applicability of normal gravity material screening methods.

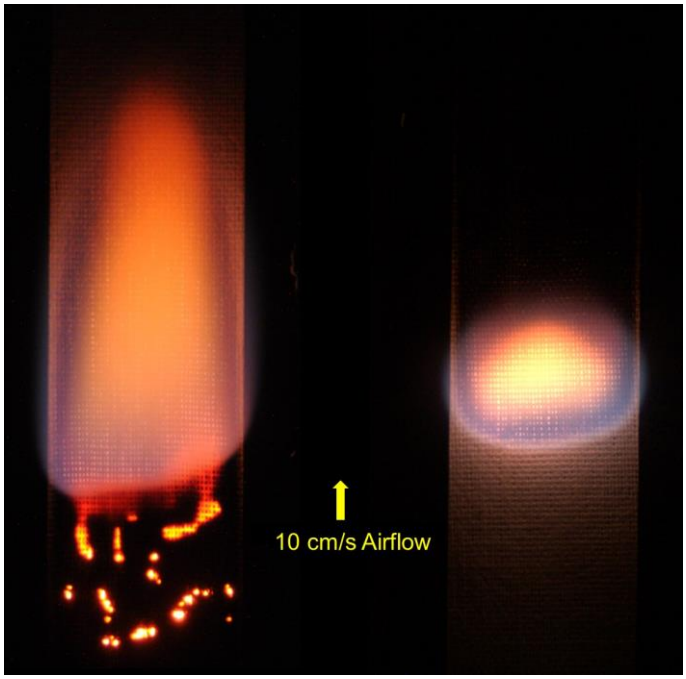

Figure 12. Concurrent and opposed comparison at 10 cm/s air flow speed. Left: Concurrent flow: Steady flame base spread rate is 2.55 mm/s. Right: Opposed flow: Steady flame spread rate is 1.21 mm/s. (Tests 7 and 6)

The fuel used in this investigation cannot burn in the downward (opposed-flow) configuration in normal gravity. Ignition can be achieved, but for any fuel width the flame will only spread downward for a short time before extinguishing. But in microgravity, this fuel will support opposed-flow burning in microgravity. The comparison is shown in Fig. 14. On the left, the opposed-flow flame in microgravity steadily and vigorously burns all the available fuel. On the right, the normal-gravity, downward-burning flame is ignited, but sputters and then goes out. The explanation is that in normal gravity, the buoyant flow generated by the flame is too high for the flame to be supported and blowoff occurs. This can be seen by referring back to Fig. 1 as the flame in normal gravity lies to the right of the flammability boundary. By going to microgravity and imposing opposed-flow speeds below the blowoff limit, the consequence is to move the system within the boundary so that the flame can be maintained. Normal gravity results cannot always be used to predict flame behavior and material flammability in spacecraft.

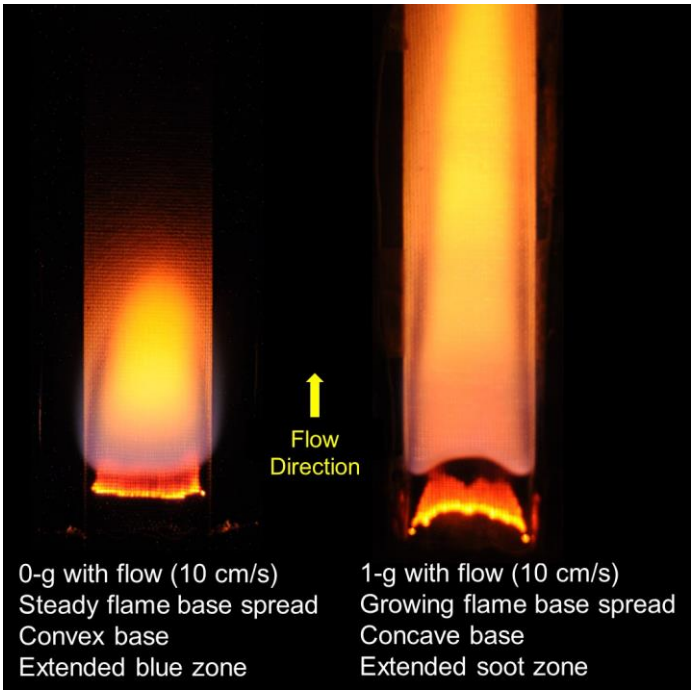

Figure 13. Comparison of 0-g concurrent-flow flame (left) and 1-g upward flame (right) for 2-cm wide sample.

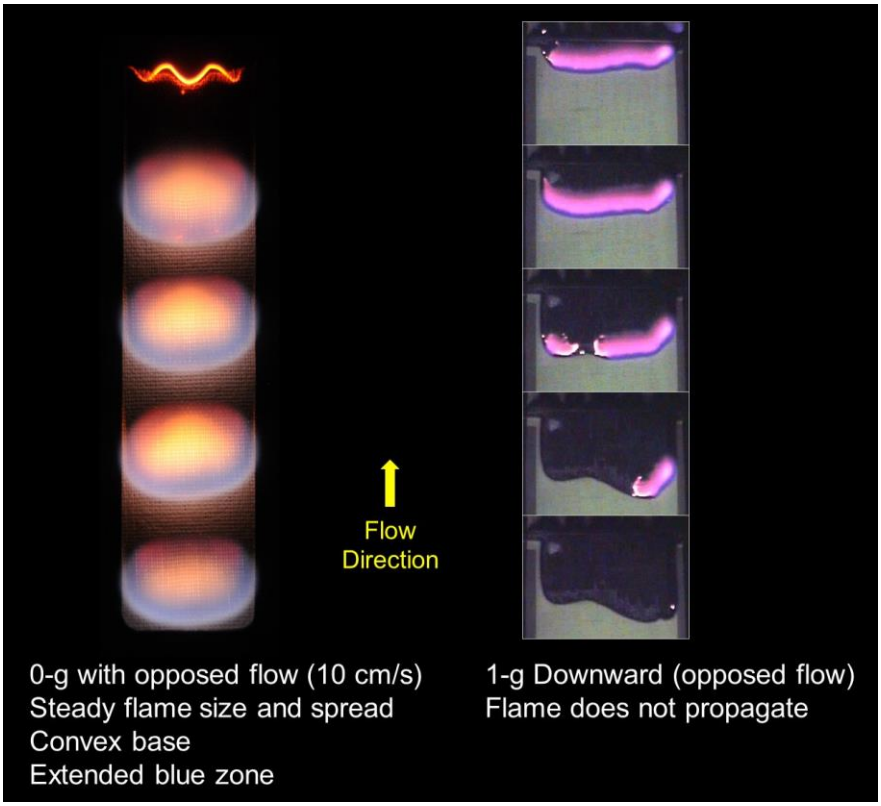

Figure 14. Comparison of 0-g and 1-g flames in opposed flow. Image sequences shows flames spreading from top down. (Test 6 and a 1-g test)

4. Conclusions

Flat fabric samples were burned in long-duration microgravity tests aboard the ISS. The samples were burned in both the opposed and concurrent-flow configurations. The custom-made cotton-fiberglass fabric performed very well, with none of the complications caused by the burnout of ordinary cellulosic fuel samples like paper. The main variable was air flow speed and it had a major effect on the flame as suggested in earlier studies.

This is the first time that detailed transient flame growth data was obtained in purely forced flows in microgravity for a thin fuel with uniform burnout characteristics. In addition, by decreasing concurrent-flow speed to a very low value (around 1 cm/s), quenching extinction was observed providing a direct verification of the theoretically predicted U-shaped flammability boundary for a thin fuel.

For the opposed flow configuration, the flame quickly reached steady spread for each flow speed, and the spread rate was fastest at an intermediate value of flow speed. These tests show the enhanced flammability in microgravity for this geometry, since, in normal gravity air, a flame self-extinguishes in the opposed-flow geometry (downward flame spread).

For the concurrent-flow configuration, a limiting length and steady spread rate were obtained only in low flow speeds. However, flame base spread rate was constant and increased linearly with increasing flow for all tests.

The valuable results from these long-duration experiments validate a number of theoretical predictions and also provide the data for a transient flame growth model under development.

Acknowledgements

This research was supported by the NASA Space Life and Physical Sciences Research and Applications Division (SLPSRA). The experiments were supported by Fumiaki Takahashi, Jay Owens, Chuck Bunnell, Tibor Lorik, Dennis Siedlak, and Carol Reynolds. We also thank astronauts Don Pettit, Joe Acaba, and Suni Williams for conducting these experiments aboard the ISS.

References

Butler, C. (2008): Microgravity Science Glovebox (MSG) Investigation Interface Requirements Document, NASA George C. Marshall Space Flight Center, MSFC-RQMT-2888H, Revision H.

Dotson K.T., Sunderland P.B., Yuan Z.-G., Urban D.L. (2010): Laminar Smoke Points in Coflow Measured Aboard the International Space Station, AIAA 48th Aerospace Sciences Meeting and Exhibit, Orlando, FL.

Ferkul, P. V. and T'ien, J. S. (1994): A Model of Low-Speed Concurrent Flow Flame Spread Over a Thin Solid, Combustion Science and Technology, Vol. 99, pp. 345-370.

Grayson, G. D., Sacksteder, K. R., Ferkul, P. V., and T'ien, J. S. (1994): Flame Spreading Over a Thin Solid in Low-Speed Concurrent Flow - Drop Tower Experimental Results and Comparison with Theory, Microgravity Science and Technology, VII/2, pp. 187-195.

NASA (1998): Flammability, Odor, Offgassing, and Compatibility Requirements and Test Procedures for Materials in Environments that Support Combustion, NASA STD 6001, Test 1, Upward Flame Propagation (formerly NHB 8060.1C).

Olson, S.L., (1991): Mechanisms of Microgravity Flame Spread Over a Thin Solid Fuel: Oxygen and Opposed Flow Effects, *Combustion Science and Technology*, 76, 4-6, pp. 233-249.

Olson, S. L., Ferkul, P. V., and T'ien, J. S. (1988): Near Limit Flame Spread Over a Thin Solid Fuel in Microgravity, 22nd Symposium (International) on Combustion, The Combustion Institute, pp. 1213-1222 and NASA TM 100871.

Olson, S. L., Kashiwagi, T., Fujita, O., Kikuchi, M., and Ito, K. (2001): Experimental Observations of Spot Radiative Ignition and Subsequent Three-Dimensional Flame Spread Over Thin Cellulose Fuels, Combustion and Flame, Vol. 125, No. 1/2, pp. 852-864.

Sacksteder, K. R., T'ien, J. S., Greenberg, P. S., Ferkul, P. V., Pettegrew, R. D., and Shih, H. Y. (1997): Forced Flow Flame Spreading Test: Preliminary Findings from the USMP-3 Shuttle Mission, Joint Launch Plus One Year Review of USML-2 and USMP-3, NASA Conference Publication.

Shih, H.-Y. and T'ien, J. S. (1997): Modeling Wall Influence on Solid-Fuel Flame Spread in a Flow Tunnel, Paper AIAA-97-0236, presented at the AIAA 35th Aerospace Sciences Meeting.

T'ien, J. S. and Bedir, H. (1997): Radiative Extinction of Diffusion Flames - A Review, Asia-Pacific Conference on Combustion, Osaka, Japan.